

SAND TRANSPORT IN PROCTOR CRATER ON MARS BASED ON DUNE MORPHOLOGY AND MESOSCALE MODELING. L. K. Fenton¹, M. I. Richardson¹, and A. D. Toigo², ¹California Institute of Technology, MS 150-21, Pasadena, CA, 91125, lori@gps.caltech.edu, mir@gps.caltech.edu, ²Cornell University, Space Sciences Bldg., Ithaca, NY, 14853, toigo@astro.cornell.edu.

Introduction: Aeolian action is most likely the dominant geological process currently acting on the surface of Mars. The ubiquitous dunes, yardangs, deflation pits, dust storms, and dust deposits of low thermal inertia are indicators of the impact that aeolian weathering has had throughout Mars' geological past. Ventifacts, sand drifts, and rock windtails at the Viking and Mars Pathfinder landing site are small-scale products of aeolian activity at the surface [1, 2]. A disparity in the orientations of these features at the Mars Pathfinder landing site has led to the conclusion that the wind circulation pattern in the region, as well as the type and magnitude of aeolian activity, has undergone a dramatic shift [3, 4, 5]. Recent studies of the Martian surface from the equatorial region [6] to the northern polar deposits [7] have revealed a complex history of aeolian deposition and erosion that is likely global in extent. Aeolian processes may well dominate the stratigraphic record on Mars, revealing the climatic conditions and the sedimentary environment of the last few billion years of Mars' history.

Sand dunes have the unique capacity of recording their sedimentary history in a way that can be identified in spacecraft imagery. A sand dune slipface indicates the direction of the wind that last influenced its morphology. Thus, stabilized or cemented dunes reflect the wind regime and climate, and they can be compared to active dunes and the current wind patterns. In addition, sand accumulations upwind or downwind of a dunefield can be used to identify transport pathways [8]. A dunefield may be considered a sink along a transport pathway, where sand is temporarily or permanently trapped. Once such transport pathways are located, the source location of the dune sands may be identified.

The goal of this work is to determine the recent sedimentary and climate history of Proctor Crater by studying the local sources, sinks, and transport pathways of sand. We use a twofold approach of investigating the sand deposits in Proctor Crater. First, we have identified the transport pathways and dune slipface directions using Viking and MOC images. This leads to an understanding of the complexity of the wind regime affecting the sand inside the crater. Second, we have applied a mesoscale model (the Mars MM5) over Proctor Crater to compare the current wind regime to the wind patterns recorded in the dunes. Thus, the model is used as a tool to place constraints on the age of dune slipfaces. Used in concert, these two methods provide a

comprehensive approach to determining the climate change and sedimentary history on Mars.

Study Area: Proctor Crater (see Fig. 1) is located in the Southern Highlands of Mars, at a latitude of 45° S. It is one of many old craters in the area west of Hellas Planitia that contain a prominent, dark dunefield. The dunes of Proctor Crater (like most of the large dunes on Mars) are traditionally considered to be transverse. We chose Proctor Crater as a study area because its dunefield has been used as a type example for dune activity [9], terrestrial analog studies [10], and thermal properties of sand [11, 12].

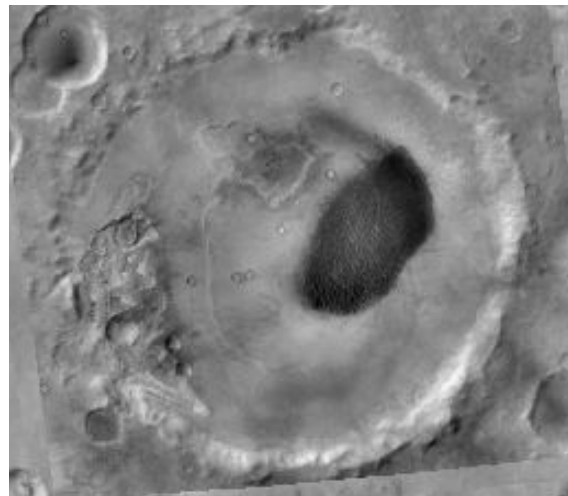


Figure 1. MOC WA image of Proctor Crater and dunefield

Surficial Mapping: To best study the morphology and distribution of sand dunes in the crater, both MOC Narrow Angle and high-resolution Viking images were superimposed on a MOC Wide Angle mosaic. Only the MOC Narrow Angle images had the necessary resolution to distinguish dune slipfaces and sand accumulations beyond the main dunefield. These images were used to map dune crests and outliers of sand, with interpretations made to the low-resolution base image where possible.

The mapping of outliers revealed a region on the floor of the crater and southwest of the dunefield where sand has accumulated on the northeastern side of craters, hills, and cliffs. Because many of these features appear to extend some distance from the obstacles, we interpret them as lee dunes and falling dunes formed from a southwesterly wind.

In the main dunefield, the brinks of dune slipfaces were mapped and measured for orientation (see Fig. 2). The small bright duneforms and boulders in Figure 2 lie stratigraphically beneath the large dark dunes. Two main slipface orientations were discovered, indicating that the dunes of Proctor Crater reside in a bi-directional wind regime. The average orientation (where 0° refers to winds from the north) of the sharper and more prevalent slipfaces, and thus the primary wind, is $246^\circ \pm 15^\circ$ (in yellow in Fig. 2), and the average orientation of the secondary wind is $100^\circ \pm 22^\circ$ (in blue in Fig. 2). Upon close inspection of the center of the dunefield, the dunes do indeed resemble reversing transverse dunes.

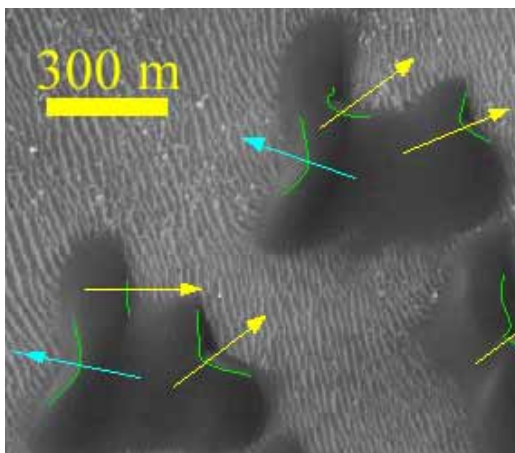


Figure 2. Slipface brink orientations

Mesoscale Model: To model the winds over the Proctor Crater dunefield, we applied the Mars MM5 (Mesoscale Model Version 5), developed from the PSU/NCAR MM5 [13]. The Mars MM5 uses boundary and initial conditions provided by the GFDL Mars GCM [14]. It is nonhydrostatic, uses terrain-following sigma-coordinates, and applies the same radiation scheme as the GFDL Mars GCM. Recent topography, albedo, and thermal inertia maps are used to model the surface. The model uses a boundary layer scheme from the Medium Range Forecast (MRF) to represent transfer of momentum from the atmosphere to the surface.

We ran the model for seven ten-day time periods distributed through the Martian year. We used 24 vertical levels from the surface to ~ 50 km and a horizontal spatial resolution of 10 km. The model timestep was 5 sec, although data output was recorded 12 times each day (every 2 hours).

Results: The goal of applying a mesoscale model to the study area is primarily to determine if winds above the saltation threshold for sand exist in the current wind regime on Mars, and if they are present, to determine how well they correlate with dune slipface

orientations. To determine which modeled wind stresses rose above the saltation threshold for sand, we used an empirically derived relation [15] using $100 \mu\text{m}$ quartz particles at $T=200$ K and $p=550$ Pa.

Figure 3 shows a plot of wind orientation vs. L_s . The seven modeled L_s periods are shown in blue, with black X's marking the orientation of surface winds located on the dunefield that have stresses above the saltation threshold. In red on the plot are the orientations of the primary and secondary winds. The primary dune-forming winds match up well with fall and winter winds caused by mid-latitude westerlies enhanced by thermal contrast from the nearby seasonal polar cap. The secondary dune-forming winds correlate best with easterlies caused by the summer thermal gradient reversal, and are weaker than the primaries because the seasonal polar cap is no longer present.

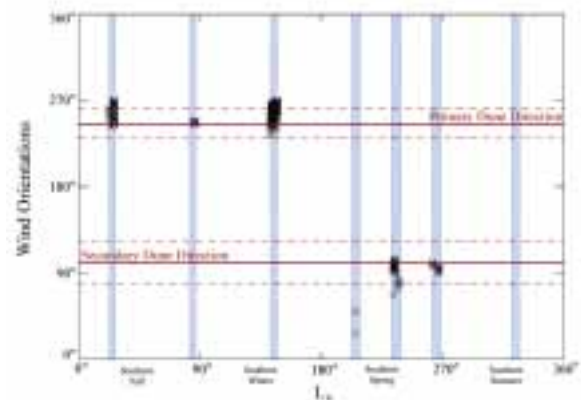


Figure 3. Comparison of model winds with slipface orientations.

Conclusions: Both high-resolution imagery and mesoscale modeling indicate that the dunes of Proctor Crater are not the simple transverse dunes as they have always appeared. Now they may be relabel them as a combination of reversing transverse and multidirectional dunes that match the circulation patterns of the current wind regime.

References: [1] Mutch T. A. et al. (1977) *JGR*, 82, 4452-4467. [2] Greeley R. et al. (1999) *JGR*, 104, 8573-8584. [3] Greeley R. et al. (2000) *JGR*, 105, 1829-1840. [4] Bridges N. T. et al. (1999) *JGR*, 104, 8595- 8615. [5] Fenton L. K. and Richardson M. I. (2002) *JGR*, in press. [6] Zimbelman J. R. (2001) *AGU Abst.*, P42A-0560. [7] Byrne S. and Murray, B. C. Submitted to *JGR*. [8] Zimbelman J. R. et al. (1995) In *Desert Aeolian Processes*, 101-130. [9] Edgett K. S. and Malin M. C. (2000) *JGR*, 105, 1623-1650. [10] Breed C. S. (1977) *Icarus*, 30, 326-340. [11] Edgett K. S. and Christensen P. R. *JGR*, 99, 1997-2018. [12] Herkenhoff K. E. and Vasavada A. R. *JGR*, 104, 16,487-16,500. [13] Toigo, A. D. (2001) Ph.D. Thesis, Calif. Inst. of Tech., 139 pp. [14] Wilson R. J. and Hamilton K. (1996) *JAS*, 53, 1290-1326. [15] Iversen J. D. and White B. R. (1982) *Sediment.*, 29, 111-119.